ISSN 1 746-7233, England, UK
World Journal of Modelling and Simulation
Vol. 9 (2013) No. 1, pp. 59-67

Direct torque control of induction motor fed by two level inverter using space vector pulse width modulation

Y. Srinivasa Kishore Babu[1*] , G. Tulasi Ram Das[2]

[1] School of Electrical Engineering, Vignan University, Guntur 522213, India
[2] Vice-Chancellor of Jawaharlal Nehru Technological University, Kakinad Kakinad, India

(*Received July 26 2012, Accepted November 20, 2012*)

Abstract. This paper presents the application of Space Vector Pulse Width Modulation (SVPWM) technique to reduce torque ripple in an induction motor employing Direct Torque Control (DTC). The effective time is determined using imaginary time vector there by the lengthy procedure of using reference voltage vector is eliminated. Also the sector identification and angle determination are not used. Simulation studies have been carried out for proposed method and results are compared with the classical DTC .The results shows that the torque, current and flux waveforms are superior to that of classical DTC. The performance of the drive system is evaluated through digital simulation using MATLAB-SIMULINK package.

Keywords: direct torque control (DTC), space vector pulse width modulation (SVPWMM), induction motor

1 Introduction

The Induction Motor (IM) drives controlled with the vector control method has found wide acceptance in the industry. Sensorless control of induction motor drive has received wide attention in the industry in last one decade[12]. This is due to the various advantages associated with induction motor such as less maintenance, simple and rugged construction and simultaneously the development of less expensive and fast DSP controllers. The progress of sensorless drives can be considered to have begun around three decade ago by Blaschke[1].However; this control technique requires complex coordinate transformation, inner current control loop and accurate system parameters. On the other hand Direct Torque Control (DTC) by Takahashi [13] for low and medium power application and direct self-control by Depenbrock [6] for high power application are the two strategies increasingly being used in the industry. In DTC, torque and flux are controlled independently by selecting the optimum voltage space vector for the entire switching period and the errors are maintained with in the hysteresis band. For the small hysteresis band, frequency of operation of PWM inverter could be very high. The switching frequency always varies according to the width of hysteresis band. Though DTC has high dynamic performance, it has few drawbacks such as: Vibrations and acoustic noise due to torque ripple, harmonics and power loss due to current and flux ripple and Variation in switching frequency of the PWM inverter. Effects of torque and flux hysteresis band amplitudes on the performance of induction motor are studied in [3] while its analytical investigation is given in [4]. Torque ripple can be minimized using the method proposed in [10] but flux and current ripples are further deteriorated. Flux and current waveforms can be improved by the method proposed in [7–9] called space vector pulse width modulation (SVPWM). One of the basic aims, the simplicity of DTC is lost in the above techniques. Many other schemes of DTC presented in the literature are highly complex and does not qualify the definition of DTC[2].

In this paper a scheme has been proposed, by which, the ripples can be reduced by a considerable amount and more importantly the algorithm for this technique is quite simpler. The switching patterns and results are

* Corresponding author. *E-mail address*: yskbabu@gmail.com.

similar to SVM DTC. But it does not require the angle and sector identification and also the look up table, thus reduces the burden on the processor. Simulation is carried out in MATLAB environment and results are compared with classical DTC. It shows that this technique poses superiority than the classical one[13].

The complete paper is organized as follows: Section II explains the mathematical modeling of induction motor. Section III discusses the SVPWM and concept of imaginary switching time. The simulation results, comparison and discussion are presented in Section IV. Section V concludes the work.

2 Mathematical modeling of induction motor

In DTC the induction motor is modeled in stationary reference frame, thus it does not require any transcendental equations as they require in Field Oriented Control[13]. Stator and rotor fluxes can be expressed as follows.

$$\begin{aligned}
&\lambda_{sD} = \int \left(v_{sD} - R_s \dot{i}_{sD}\right)\mathrm{d}t,\ \lambda_{sQ} = \int \left(v_{sQ} - R_s \cdot i_{sQ}\right)\mathrm{d}t,\\
&\lambda_{rD} = \int \left(v_{rD} - R_r \cdot i_{rD} - P \cdot \omega_m \cdot \lambda_{rQ}\right)\mathrm{d}t = \int \left(-R_r \cdot i_{rD} - P \cdot \omega_m \cdot \lambda_{rQ}\right)\mathrm{d}t,\\
&\lambda_{rQ} = \int \left(v_{rQ} - R_r \cdot i_{rQ} + P \cdot \omega_m \cdot \lambda_{rD}\right)\mathrm{d}t = \int \left(-R_r \cdot i_{rQ} + P \cdot \omega_m \cdot \lambda_{rD}\right)\mathrm{d}t.
\end{aligned} \tag{1}$$

[For squirrel cage induction motor $v_{rD} = v_{rQ}$=0].

Stator and rotor flux linkage equation can be written as follows:

$$\lambda_{sQ} = L_s i_{sQ} + L_m i_{rQ},\ \lambda_{sD} = L_s i_{sD} + L_m i_{rD},\ \lambda_{rQ} = L_r i_{rQ} + L_m i_{sQ},\ \lambda_{rD} = L_r i_{rD} + L_m i_{sD}. \tag{2}$$

Solving the upper set of equations the stator and rotor current equations are derived as follows:

$$i_{sD} = \lambda_{sD} \cdot \frac{L_r}{L_x} - \lambda_{rD} \cdot \frac{L_m}{L_x},\quad i_{sQ} = \lambda_{sQ} \cdot \frac{L_r}{L_x} - \lambda_{rQ} \cdot \frac{L_m}{L_x}, \tag{3}$$

$$i_{rD} = \lambda_{rD} \cdot \frac{L_s}{L_x} - \lambda_{sD} \cdot \frac{L_m}{L_x},\quad i_{rQ} = \lambda_{rQ} \cdot \frac{L_s}{L_x} - \lambda_{sQ} \cdot \frac{L_m}{L_x}, \tag{4}$$

where $L_x = L_s.L_r - L_m^2$.

Electromagnetic torque expression of machine is as follows:

$$T_e = \frac{3}{2} P \left[\lambda_{sD} \times i_{sQ} - \lambda_{sQ} \times i_{sD}\right]. \tag{5}$$

The speed can be calculated from the following:

$$T_e - T_L = J\frac{d\omega_m}{dt} + B\omega_m. \tag{6}$$

3 Space vector modulation (SVM) & concept of imaginary switching

The space vector modulation (SVM) method is an advanced, computation- intensive Pulse Width Modulation (PWM) method and is possibly the best among all the PWM techniques for variable-frequency drive application. Because of its superior performance characteristics, it has been finding widespread application in recent years. The SVM method considers the interaction of the phases and optimizes the harmonic content of the three phase isolated neutral load. To understand the SVM theory, the concept of a rotating space vector is very important. If the three phase sinusoidal and balanced voltages are applied to a three-phase induction machine, it can be shown that the space vector V^* rotates in a circular orbit at angular velocity where the

direction of rotation depends upon the phase sequences. With the sinusoidal three-phase command voltages, the composite PWM fabrication at the inverter output should be such that the average voltages follow these command voltages with a minimum amount of harmonic distortion.

The modulating command voltages of a three-phase inverter are always sinusoidal and therefore they constitute a rotating space vector V^*, as shown in Fig. 1. For the location of the V^* vector shown in Fig. 1, as an example a convenient way to generate the PWM output is to use the adjacent vectors $V_1$and V_2 of sector 1 on a part time basis to satisfy the average output demand. The V^* can be resolved as follows:

$$V^* \sin(\frac{\pi}{3} - \alpha) = V_a \cdot \sin\frac{\pi}{3}, \quad V^* \sin\alpha = V_b \cdot \sin\frac{\pi}{3}, \tag{7}$$

$$V_a = \frac{2}{\sqrt{3}} \cdot V^* \cdot \sin(\frac{\pi}{3} - \alpha), \quad V_b = \frac{2}{\sqrt{3}} \cdot V^* \cdot \sin\alpha, \tag{8}$$

where $V_a$and V_b are the components of V^* aligned in the direction of V_1 and $V_{2,}$ respectively. Considering the sampling period T_{ss} during which the average output should match the command, it can be written as:

$$V^* = V_a + V_b = V_1 \cdot \frac{T_1}{T_{ss}} + V_2 \cdot \frac{T_2}{T_{ss}} + (V_0 or V_7) \cdot \frac{T_0}{T_{ss}}, \quad V^* \cdot T_{ss} = V_1.T_1 + V_2 \cdot T_2 + (V_0 or V_7) \cdot T_0, \tag{9}$$

where,

$$T_1 = T_{ss} \cdot a \cdot \frac{\sin(\frac{\pi}{3} - \alpha)}{\sin 60^0}, \tag{10}$$

$$T_2 = T_{ss} \cdot a \cdot \frac{\sin\alpha}{\sin 60^0}. \tag{11}$$

The time T_1 and T_2 satisfy the command voltage while time to fills up the gap for T_{ss} with the zero or null vector. The null time has been conveniently distributed between the V_0 and V_7vectors to describe the Symmetrical pulse widths.

Here, $a = (V^*/V_1) = (V^*/V_2)$, T_{ss} = sampling time, T_1, T_2 and T_0 are the duration for which V_1, V_2 and V_0 or V_7 are applied, α is the angle of V^* with d-axis and $V_1 = V_2 = 2/3(V_{DC})$. In order to minimize the switching frequency of the power semiconductor devices in the inverter, it is desirable that switching takes place in one phase of the inverter only for a transition from one state to another. For the situation depicted in Fig. 1. (i.e. when the sample is in sector 1), this objective is met if the switching sequence (0-1-2-7-2-1-0-1-2-7 ...) is used. Therefore the zero intervals T_0 is divided into two equal halves of length $T_0/2$. These half-intervals are placed at the beginning and end of every sampling interval. One of the important advantages of the SVPWM over the Sinusoidal Pulse Width Modulation is that it gives nearly 15% more output voltage compared to the latter, while still remaining in modulation. SVPWM can also be regarded as the carrier based PWM technique with the modification that, the reference waveform has triplen harmonics in addition to the fundamental. Therefore, owing to this basic approaching manner of the classical SVM method, the overall process of this algorithm is complex and the implementation is formidable. A simple and elegant algorithm is presented in this section, which does not require the sector information and the angle (the angle subtended by the reference vector with respect to the beginning of the sector in which the tip of the reference vector is situated). This proposed algorithm is based on the instantaneous reference values of the phase voltages only. This algorithm is based on the concept of "Effective time" which is the time duration for which the load is connected to the supply. The algorithm reduces the execution time by more than 25% while the memory requirement is reduced to 15% compared to the conventional PWM method. The task of generating the gating signals is accomplished naturally and automatically with this algorithm. In this scheme, a space vector based PWM strategy is proposed based on instantaneous values of the reference values of the three phases only. This method does not depend on the magnitude of the reference voltage space vector and its relative angle with respect to the reference axis. If Eqs. (10) and (11) are simplified in terms of instantaneous phase values corresponding to its reference voltage vector, these are given by:

$$T_1 = T_{ss}\frac{V^*}{\frac{2}{3}V_{DC}}\frac{\sin(60^0-\alpha)}{\sin 60^0} = T_{ss}\frac{V^*}{V_{DC}}[2\sin 60^0\sin(60^0-\alpha)]$$
$$= T_{ss}\frac{V^*}{V_{DC}}[\cos\alpha - \cos(120^0-\alpha)] = T_{ss}\frac{V^*_{sa}}{V_{DC}} - T_{ss}\frac{V^*_{sb}}{V_{DC}}, \tag{12}$$

or

$$T_1 = T_{sa} - T_{sb}.$$

and

$$T_2 = T_{ss}\frac{V^*}{\frac{2}{3}V_{DC}}\frac{\sin\alpha}{\sin 60^0} = T_{ss}\frac{V^*}{V_{DC}}[2\sin 60^0\sin\alpha] = T_{ss}\frac{V^*}{V_{DC}}[\cos(\alpha-60^0) - \cos(\alpha+60^0)$$
$$= T_{ss}\frac{V^*}{V_{DC}}[\cos(120^0-\alpha) - \cos(240^0-\alpha) = \frac{V^*_{sb}}{V_{DC}}T_{ss} - \frac{V^*_{sc}}{V_{DC}}T_{ss}, \tag{13}$$

or

$$T_2 = T_{sb} - T_{sc},$$

where

$$T_{sa} = \frac{V^*_{sa}}{V_{Dc}}T_{ss},\ \ T_{sb} = \frac{V^*_{sb}}{V_{Dc}}T_{ss}\ \ \&\ \ T_{sc} = \frac{V^*_{sc}}{V_{Dc}}T_{ss}, \tag{14}$$

are defined as three Imaginary switching times. The value of these three times could be negative as it depends on the reference stator phase voltages V^*_{sa}, V^*_{sb} and V^*_{sc} derived from the reference phase voltage vector V^*. Extending this procedure for the other sectors, the active vector switching T_1 and T_2 for the respective sectors may be expressed in terms of the imaginary switching times T_{sa}, T_{sb} and T_{sc} for a particular sampling interval. The complete algorithms for generating the switching signals are explained in next section.

Like classical DTC technique, here also the actual stator flux vector (both d and q axis component) and electromagnetic torque are derived from motor itself either by measuring any two phase voltage and currents or by measuring the dc link voltage and any two phase currents. As torque error is proportional to slip speed which when added to motor speed gives synchronous speed. The phase angle of flux vector is determined by integrating the synchronous speed. Reference Flux space vector (both d and q axis component) derived from the torque error and motor speed.

The error between this two flux vectors generates the fictitious imaginary switching time reference vector. The d-q components of imaginary time vector are determined by the following procedure:

Stator voltage equation in d-q stationary reference frame can be written:

$$V_s = R_s \cdot i_s + \frac{d\lambda_s}{\mathrm{d}t}. \tag{15}$$

Neglecting the stator resistance, it can be simplified as:

$$\Delta\lambda_s = V_s \cdot \Delta t,\ \text{or}\ \Delta\lambda_{sd} + j\cdot\Delta\lambda_{sq} = (V_{sd} + j\cdot V_{sq})\cdot\Delta t. \tag{16}$$

Comparing the real and imaginary part of Eq. (16) gives:

$$V_{sd} = \frac{\Delta\lambda_{sd}}{\Delta t} = \frac{\lambda^*_{sd} - \lambda_{sd}}{\Delta t}, \tag{17}$$
$$V_{sq} = \frac{\Delta\lambda_{sq}}{\Delta t} = \frac{\lambda^*_{sq} - \lambda_{sq}}{\Delta t}, \tag{18}$$

where Δt is the sampling time T_{ss}.Therefore imaginary switching times in d-q stationary reference frame are calculated as follows:

$$T_{sd} = \frac{V_{sd}}{V_{DC}} \cdot T_{ss} = \frac{\Delta\lambda_{sd}}{\Delta t(= T_{ss}) \times V_{DC}} \cdot T_{ss} = \frac{\lambda^*_{sd} - \lambda_{sd}}{V_{DC}}, \tag{19}$$

$$T_{sq} = \frac{V_{sq}}{V_{DC}} \cdot T_{ss} = \frac{\Delta\lambda_{sq}}{\Delta t(= T_{ss}) \times V_{DC}} \cdot T_{ss} = \frac{\lambda^*_{sq} - \lambda_{sq}}{V_{DC},} \tag{20}$$

and

$$T_s = T_{sd} + j \cdot T_{sq} = \frac{V_{sd}}{V_{DC}} \cdot T_{ss} + j \cdot \frac{V_{sq}}{V_{DC}} \cdot T_{ss}, \tag{21}$$

$$T_s = \frac{V_s}{V_{DC}} T_{ss} = \frac{\lambda^*_s - \lambda_s}{V_{DC}}. \tag{22}$$

Therefore a new concept of imaginary switching time vector is introduced according to Eq. (22) that is directly responsible for calculating the actual switching instants of the inverter. In any case the magnitude of imaginary time vector cannot be greater than the sampling time. Component of imaginary time vector can be converted into three phase using 2-to-3-phase conversion that gives imaginary switching times T_{sa}, T_{sb} and T_{sc}. From imaginary switching times, actual times are determined as explained in the algorithm[5, 11]. These times are determined in each sampling period and accordingly the switching instants for the PWM inverter are generated. Hence torque and flux errors are compensated in each sampling interval. This improves the torque and flux waveforms. After each sampling interval, actual stator flux vector λ_s is corrected by the error and it tries to attain the reference flux space vector λ^*_s. Flux error is minimized in each sampling interval. While the speed of the reference stator flux takes care of torque demand because it is the addition of slip speed derived from the torque error and actual rotor speed. The d-q components of imaginary switching time are derived by Eq. (19) and Eq. (20). This method eliminates the requirement of sector and angle identification, which further reduces the complexity.

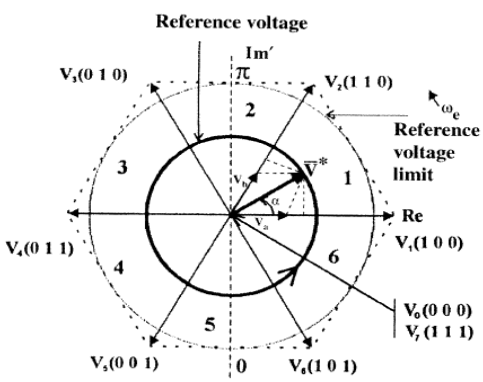

Fig. 1. Space vector of two level inverter showing reference voltage trajectory

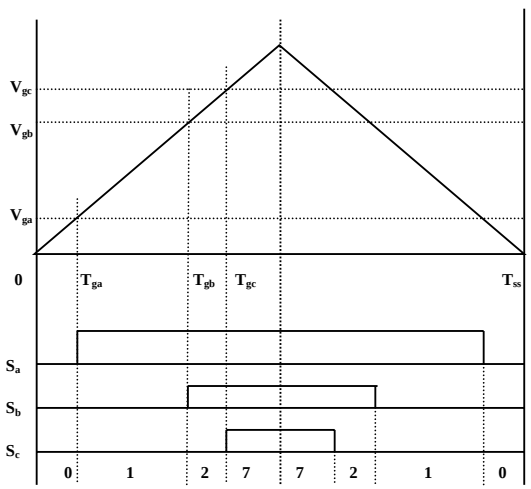

Fig. 2. Generation of pulses

Algorithm for Finding the Actual Times from Imaginary time's vector:
T Finding T_{sd} and T_{sq} by Eq. (19) and Eq. (20);
Finding T_{sa}, T_{sb} and T_{sc} by 2 to 3 phase transformations;
Finding $T_{\max} = \max(T_{sa}, T_{sb}, T_{sc})$;
Finding $T_{\min} = \min(T_{sa}, T_{sb}, T_{sc})$;
Effective Time, $T_1 + T_2 = T_{\max} - T_{\min}$;
Zero Vector Time, $T_{\text{zero}} = T_{ss} - (T_{\max} - T_{\min})$;
Finding Offset, $T_{\text{offset}} = (T_{\max}/2) + (T_{\text{zero}}/4)$;
Actual times $T_{ga} = T_{\text{offset}} - T_{sa}/2,\ T_{gb} = T_{\text{offset}} - T_{sb}/2,\ T_{gc} = T_{\text{offset}} - T_{sc}/2.$

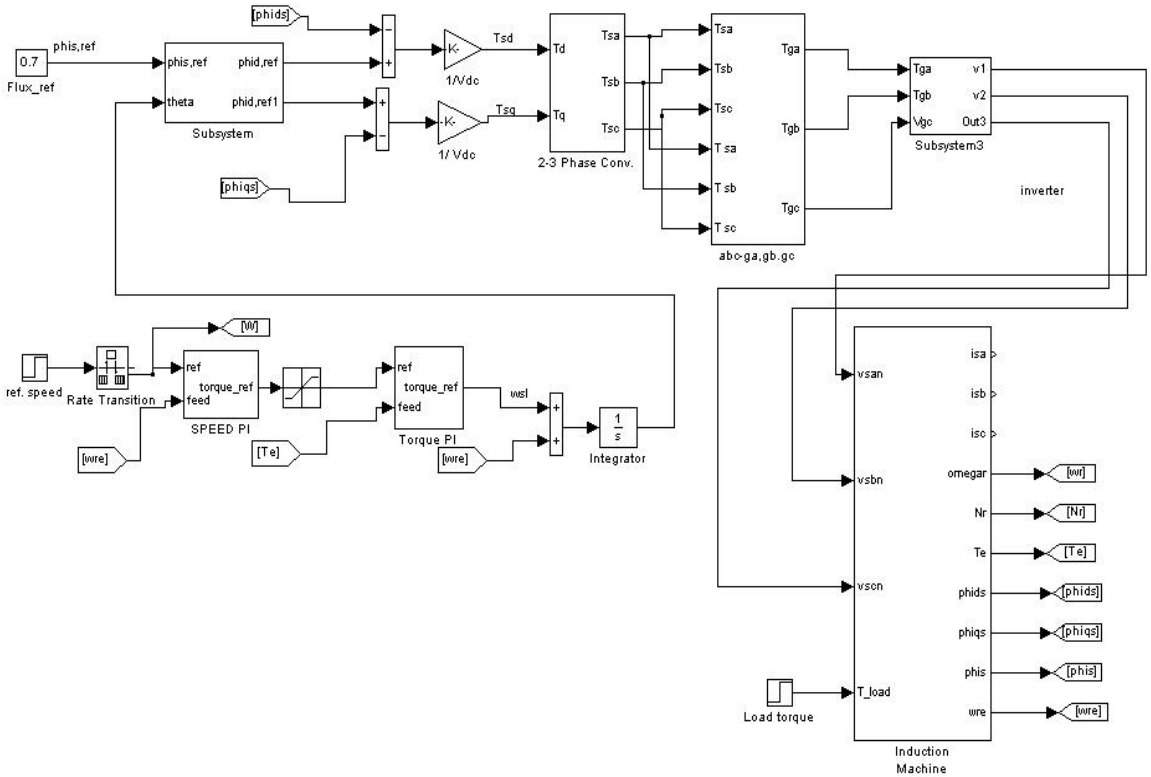

Fig. 3. Simulink diagram of SVM-DTC

From T_{ga}, T_{gb} and T_{gc} three voltages V_{ga}, V_{gb} and V_{gc} are generated. These Voltages are compared with symmetrical triangular carrier wave of frequency $1/T_{ss}$ as shown in Fig. 2. This generates the voltage for the upper switches of the inverter arm. The sequence is 0-1-2-7-7-2-1-0 as generated in the conventional SVPWM by sector and angle identification for sector 1. The Simulink model of the algorithm has been shown in the Fig. 3.

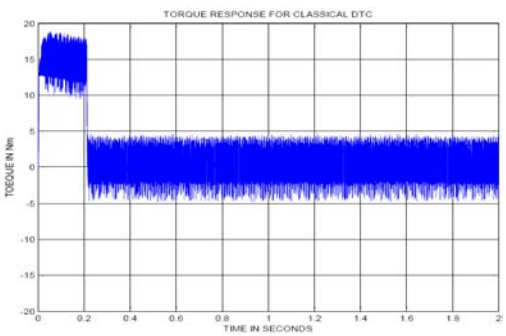

Fig. 4. Torque response at no load for classical DTC (horizontal axis-time, vertical axis-torque)

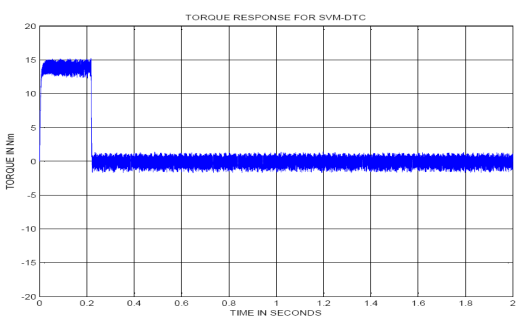

Fig. 5. Torque response at no load for SVM-DTC (horizontal axis-time, vertical axis-torque)

4 Results

A series of simulation tests are conducted on a 4KW, 4pole inverter-fed IM to evaluate the performance of proposed DTC method. Simulation studies have been carried out for the proposed and conventional methods

of direct torque control using MATLAB/SIMULINK software. Ode1 Euler's method with sampling time of 100μs is used for a fixed step size of 20μs.

Figs. 4 and 5 show the comparison result for torque response at no load condition. It can be seen that for SVM-DTC the torque ripples have been reduced significantly

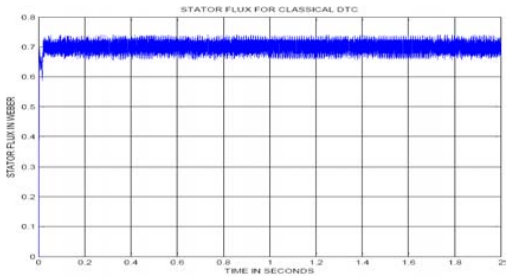

Fig. 6. Flux response at no load for classical DTC (horizontal axis-time, vertical axis-flux)

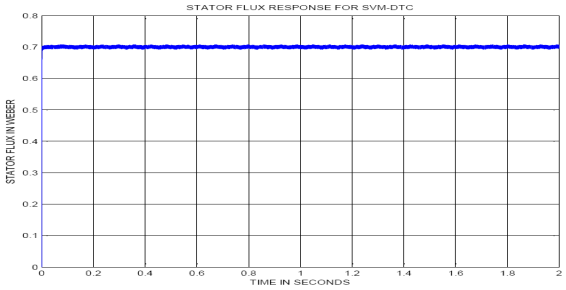

Fig. 7. Flux response at no load for SVM-DTC (horizontal axis- time, vertical axis-flux)

The above figures show the flux response for both the types of DTC with the flux reference of 0.7 Weber. The SVM technique has helped to reduce the flux ripples also.

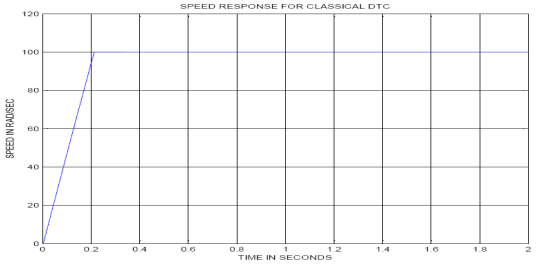

Fig. 8. Speed response at no load for Classical DTC for reference speed of 100 rad/sec

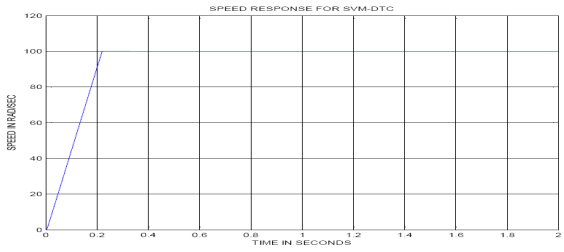

Fig. 9. Speed response at no load for SVM-DTC for reference speed of 100 rad/sec

Figs. 10 and 11 depict the situation where a speed a command of 100 rad/sec has been applied and a load of 5 Nm has been given at 1 sec. In this case also the ripples in simplified SVM-DTC is much less than the classical one.

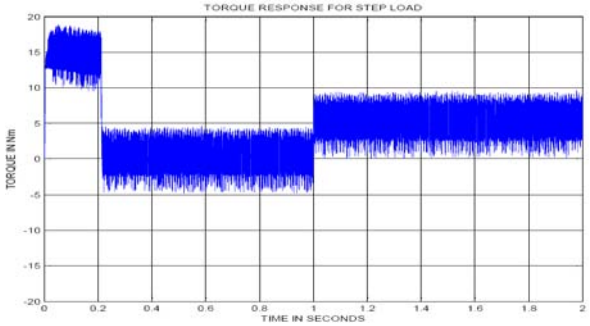

Fig. 10. Torque response for a step load of 5N-m applying at 1sec for classical DTC

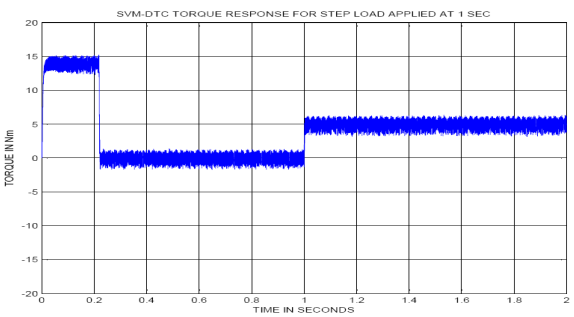

Fig. 11. Torque response for a step load of 5N-m applying at 1sec for novel SVM-DTC

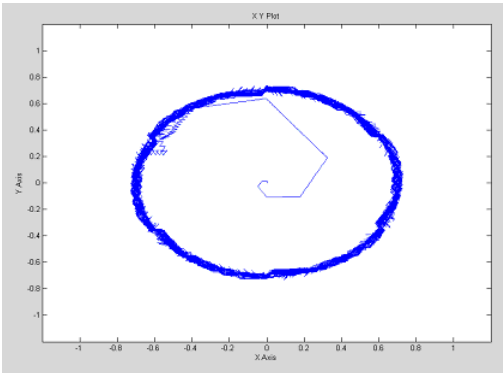

Fig. 12. Stator flux trajectory in classical DTC (horizontal axis-d axis flux linkage, vertical axis-q axis flux linkage)

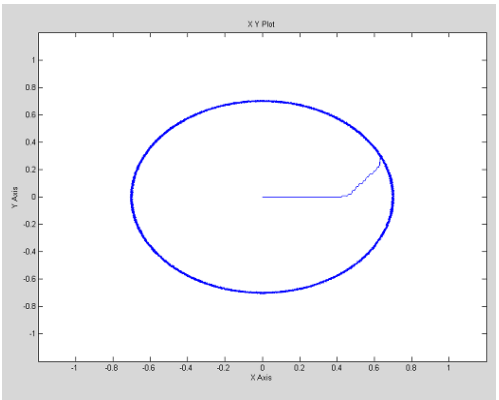

Fig. 13. Stator flux trajectory in SVM-DTC (horizontal axis-d axis flux linkage, vertical axis-q axis flux linkage)

5 Conclusions

In this paper a simplified direct torque control technique is presented. Effective time is determined using the concept of imaginary switching times. It further avoids the requirement of reference voltage vector, sector identification and angle determination. In this control strategy error between reference and estimated flux vectors is utilized to find the d-q axes imaginary switching times. This axis times can be converted into respective three imaginary switching times. These times are responsible for generating the actual voltage vector for the next switching cycle that fulfills the requirement of demanded torque and flux. This simplifies the switching technique and also retains the concept of SVPWM; either of the switching sequences (conventional or clamping) can be implemented by simply changing the offset time. Simulation studies have been carried out for both classical and simplified SVM-DTC.

Though identical results could be obtained using conventional SVM-DTC method, this simplified method requires less memory and computation time. Concept of imaginary switching vector is introduced that simplifies the calculations. Hence a very simple control strategy is developed for DTC drive of induction machine. However a time equivalent to stator resistance drop could be added while finding out the three imaginary switching times.

Appendix

3-Phase Induction Motor Parameters.
Rotor type: Squirrel cage, Reference frame: Stationary.
4KW, 1440 rpm, 50Hz, 4 Poles, R_s = 1.57Ω, R_r = 1.21 Ω, Ls = 0.17 H, L_r = 0.17 H, L_m = 0.165 H, J = 0.06 Kg-m^2.

References

[1] F. Blaschke. The principle of field-orientation as applied to the new transvector closed-loop control system for rotating-field machines. *Siemens Review*, 1972, **34**: 217–220.
[2] D. Casadei, et al. Foc and dtc: Two viable schemes for induction motors torque control. *IEEE-PE*, 2002, **17**(5): 779–786.
[3] D. Casadi, et al. Effects of flux and torque hysteresis band amplitude in direct torquecontrol of induction mache. *IEEE-IECON94*, 1994, 299– 304.
[4] D. Casadi, G. Sera, A. Tani. Analytical investigation of toque and flux ripple in dtc schemes for induction motors. *IEEE-Int. Conf. On Industrial Electronics*, 1997, **2**: 552–556.
[5] D. Chung, J. Kim, S. Sul. Unified voltage modulation technique far real-time three-phase power conversion. *EEE-IA*, 1998, **34**(2): 374–380.

[6] M. Depenbrock. Direct self control (dsc) of inverter-fed induction machine. *Power Electronics, IEEE Transactions*, 1988, **3**(4): 420–429.

[7] C. DomenicoG, G. Serra, A. Tani. Improvement of direct torque performance by using a discrete svm technique. *Power Electronics Specialists Conference*, 1998, 997–1003.

[8] T. Habelter, et al. Direct torque control of induction machines using space vector modulation. *IEEE Transaction on Industry Applications*, 1992, **28**(5): 1045–1053.

[9] T. Habetler, F. Prohmo, M. Pastorelli. Direct toque control of induction machines over a wide speed range. *Industry Applications Society Annual Meeting, 1992., Conference Record of the 1992 IEEE*, 1992, 600–606.

[10] J. Kang, S. Sul. Torque ripple minimization strategy for direct torque control of induction motor. *IEEE-IAS annual meeting*, 1998, 438–443.

[11] A. Kumar, B. Fernandes, K. Chatterjee. Simplified svpwm-dtc of 3-phase induction motor using the concept of imaginary switching times. *The 30th Annual Conference of the IEEE Industrial Electronics Society, Busan, Korea*, 2004, 341–346.

[12] K. Rajasshekara, A. Kawamura, K. Matsuse. Sensorless conml of ac motor drives-speed and position sensorless operatioq. *IEEE Press, Piscataway*, 1996.

[13] I. Takahashi, T. Noguchi. A new quick-response and high-efficiency control of induction motor. *IEEE Transaction on Industry Applications*, 1986, **IA-22**(5): 820–827.